

# Limb reduction in squamate reptiles correlates with the reduction of the chondrocranium: A case study on serpentiform anguids

Oleksandr Yaryhin<sup>1,2</sup>  | Jozef Klembara<sup>3</sup>  | Yuriy Pichugin<sup>1</sup>  |  
Marketa Kaucka<sup>1</sup>  | Ingmar Werneburg<sup>4,5</sup> 

<sup>1</sup>Max Planck Institute for Evolutionary Biology, Plön, Germany

<sup>2</sup>Schmalhausen Institute of Zoology of NAS of Ukraine, Kyiv, Ukraine

<sup>3</sup>Faculty of Natural Sciences, Department of Ecology, Comenius University in Bratislava, Bratislava, Slovakia

<sup>4</sup>Senckenberg Centre for Human Evolution and Palaeoenvironment (HEP) an der Universität Tübingen, Tübingen, Germany

<sup>5</sup>Fachbereich Geowissenschaften der Eberhard-Karls-Universität Tübingen, Tübingen, Germany

## Correspondence

Oleksandr Yaryhin, Max Planck Institute for Evolutionary Biology, August-Thienemann-Straße 2, Plön 24306, Germany.  
Email: alex.yarigin@gmail.com

Ingmar Werneburg, Senckenberg Center for Human Evolution and Palaeoenvironment (HEP) at Eberhard-Karls-Universität, Sigwartstraße 10, Tübingen 72076, Germany.  
Email: ingmar.werneburg@senckenberg.de

## Funding information

DFG-funds, Grant/Award Numbers: WE 5440/6-1, WE 5440/5-1; Slovak Ministry of Education, Grant/Award Number: 1/0228/19

## Abstract

**Background:** In vertebrates, the skull evolves from a complex network of dermal bones and cartilage—the latter forming the pharyngeal apparatus and the chondrocranium. Squamates are particularly important in this regard as they maintain at least part of the chondrocranium throughout their whole ontogeny until adulthood. Anguid lizards represent a unique group of squamates, which contains limbed and limbless forms and show conspicuous variation of the adult skull.

**Results:** Based on several emboadryonic stages of the limbless lizards *Pseudopus apodus* and *Anguis fragilis*, and by comparing with other squamates, we identified and interpreted major differences in chondrocranial anatomy. Among others, the most important differences are in the orbitotemporal region. *P. apodus* shows a strikingly similar development of this region to other squamates. Unexpectedly, however, *A. fragilis* differs considerably in the composition of the orbitotemporal region. In addition, *A. fragilis* retains a paedomorphic state of the nasal region.

**Conclusions:** Taxonomic comparisons indicate that even closely related species with reduced limbs show significant differences in chondrocranial anatomy. The Pearson correlation coefficient suggests strong correlation between chondrocranial reduction and limb reduction. We pose the hypothesis that limb reduction could be associated with the reduction in chondrocrania by means of genetic mechanisms.

## KEYWORDS

body elongation, chondrocranium, development, lepidosaurs, limb reduction, limblessness, pleiotropy, reptiles, skull

This is an open access article under the terms of the Creative Commons Attribution-NonCommercial-NoDerivs License, which permits use and distribution in any medium, provided the original work is properly cited, the use is non-commercial and no modifications or adaptations are made.

© 2021 The Authors. Developmental Dynamics published by Wiley Periodicals LLC on behalf of American Association of Anatomists.

## 1 | INTRODUCTION

On a par with the axial skeleton, the skull is the most important novelty in the evolution of vertebrates. The emergence of the skull promoted the rapid increase in the diversification of vertebrates and the conquering of new ecological “niches.” In vertebrates, the skull evolved from a complex network of cartilage—with the chondrocranium supporting the brain and the pharyngeal apparatus—and dermal bones.

In nonamniotes, the chondrocranium plays a significant role during the larval period and, in some cases, in adulthood.<sup>1–3</sup> In amniotes, the chondrocranium—evidently inherited from nonamniotes—is mainly present as a provisory organ, existing only during the embryonic period of life, and later, due to processes of endochondral ossification, becoming almost entirely replaced by bone and firmly integrated with the dermatocranium.<sup>4</sup>

Lepidosaurs are the only amniotes in which at least the anterior part of the chondrocranium, that is, the nasal capsules and a part of the orbitotemporal region, remains cartilaginous throughout ontogeny and persists into adulthood.<sup>5</sup> Recently, it has been shown that the chondrocranium plays an important biomechanical role in adults.<sup>1</sup>

The fully formed chondrocranium in lepidosaurs displays great diversity in structure and shape. Within lepidosaurs, the chondrocranium of the tuatara *Sphenodon punctatus* is the most anatomically complex<sup>6–9</sup> and snakes possess the most simplified chondrocranial anatomy, which is mainly reflected in the reduction of the orbitotemporal region.<sup>5</sup> It is worth noting that, in those clades of lizards where different grades of limb reduction are present, such as in the Geckota<sup>10–14</sup> or in the Scincoidea,<sup>15–22</sup> the chondrocranial anatomy is more variable, whereas in clades which do not show any limb rudimentation or body elongation, the chondrocranial anatomy is more consistent, for example, in the Lacertidae.<sup>23–26</sup> In this regard, Anguinae is most relevant. This clade contains 85 recent species in 11 genera.<sup>27</sup> Like skinks, they show significant limb diversity, ranging from species with well-developed limbs to species with a completely legless locomotion. Based on molecular phylogeny, anguine lizards form the sister group of varanids and, as such, they are likely the closest clade to snakes, which are also limbless.<sup>28,29</sup>

Although the adult skeletal anatomy of anguine lizards has been intensively studied,<sup>30–36</sup> little is known about the embryonic development of the skull in this enigmatic clade of lizards. The only description of a fully formed chondrocranium is available for *Anguis fragilis*.<sup>37</sup>

In the present paper, we provide the first description of the chondrocranial development in the anguine *Pseudopus apodus* and a revision of the chondrocranial anatomy of *A. fragilis*. By combining our results with existing data, we performed a correlation test which has shown a correlation between reductions in chondrocrania and limbs. Based on these results, we pose the hypothesis that limb reduction could be associated with the reduction in chondrocrania by means of genetic mechanisms.

## 2 | RESULTS

Here we mostly concentrate on some differences between the two species at the stage where the chondrocranium is fully formed, and on developmental aspects of particular structures in *Pseudopus apodus*.

### 2.1 | Chondrocranial anatomy of two anguine lizards

The chondrocranium in both species supports the well-developed brain. The brain shape is strikingly different in both lizards (Figures 1 and 2). Compared to *Anguis fragilis*, the brain in *Pseudopus apodus* at this developmental stage has more pronounced major regions and looks more elevated, the latter description pertaining particularly to the midbrain. The transition between the olfactory tract and the telencephalon is also more prominent in *P. apodus*.

The chondrocrania of both species are gracile and relatively elongated (Figures 3 and 4). The height of the chondrocranium is almost equal to the width in *A. fragilis* and slightly higher in *P. apodus*. However, the chondrocranium of *P. apodus* is nearly three times longer than width, whereas, in *A. fragilis*, the length of the chondrocranium is only twice as long as the width. Both species have a relatively elongated nasal region.

### 2.2 | Nasal region

The nasal region of the chondrocranium in both species is represented by the paired nasal capsules divided by the nasal septum. The nasal septum medially separates the paired olfactory organs (Figures 3C, 4C, and 5B,C). The ventral edge of the nasal septum bifurcates into a paired cartilaginous plate—the parietotectal cartilage. It covers the olfactory organ from above, laterally, and—by forming the cupola anterior—partially also anteriorly. The posterior portion of the parietotectal cartilage bears a

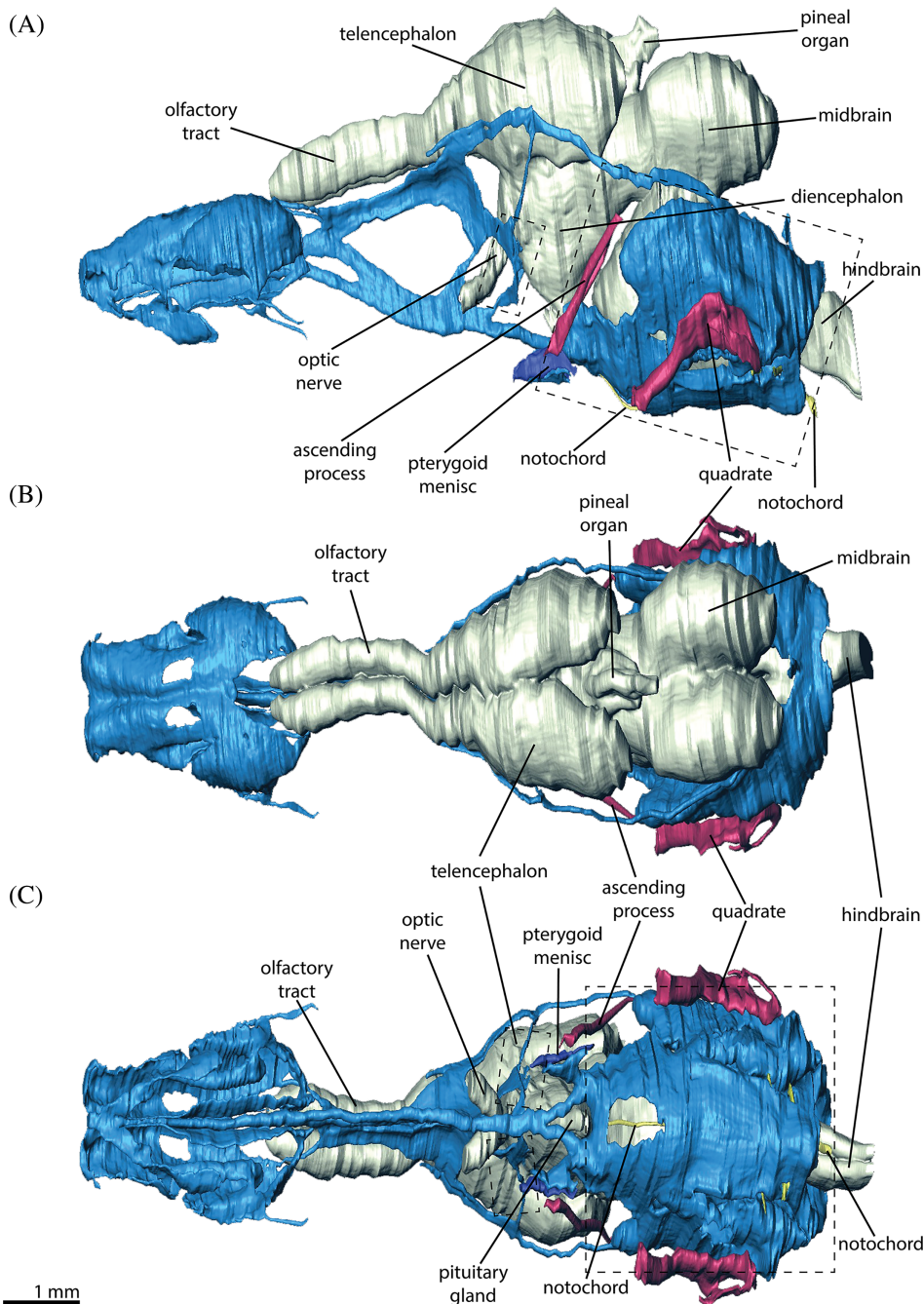


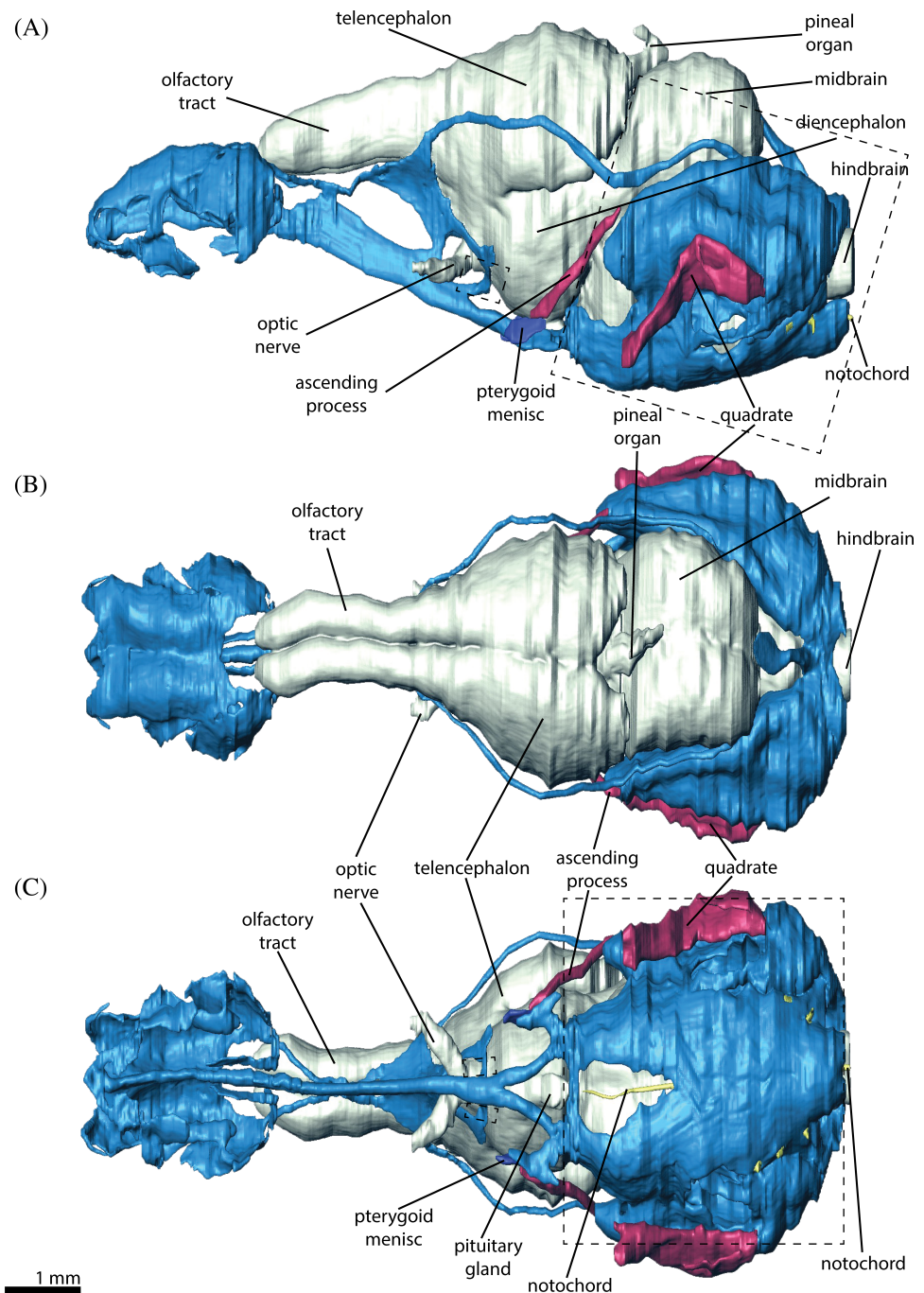
**FIGURE 1** Three dimensional reconstruction of the fully formed chondrocranium (in blue), brain (in light yellow), and the elements of the palatoquadrate (in purple) of *Pseudopus apodus* in lateral (A), dorsal (B), and ventral (C) view. Dashed line boxes indicate the parts of the chondrocranium which are of the mesodermal origin

fenestra superior, which is quite prominent in *Pseudopus apodus* and very small in *Anguis fragilis*. The anterior portion of the parietotectal cartilage has two processes: the processus alaris inferior and the processus alaris superior (Figures 3 and 4), which are well developed in both species. However, in *A. fragilis*, the processus alaris inferior is much more prominent compared to the processus alaris superior. Behind the processus alaris superior, approximately at the level of the duct of the vomeronasal organ (VNO), the parietotectal cartilage expands ventrally, where it fuses with the lamina transversalis anterior. The lamina transversalis anterior

is a slender cartilaginous plate, which anteriorly is fused with the ventral edge of the nasal septum and travels posterolaterally to support the VNO. Behind the fusion with the parietotectal cartilage, at the level of the VNO, the posterior wall of the lamina transversalis anterior continues as an ectochoanal cartilage. In *A. fragilis*, the ectochoanal cartilage only reaches the level where the nasolacrimal duct opens into the choana, while in *P. apodus* the ectochoanal cartilage spreads slightly further (Figures 3C, 4C, and 5B,C).

Posteriorly, the nasal capsule is restricted by the planum antorbitale. The planum antorbitale is a

**FIGURE 2** Three dimensional reconstruction of the fully formed chondrocranium (in blue), brain (in light yellow), and the elements of the palatoquadrate (in purple) of *Anguis fragilis* in lateral (A), dorsal (B), and ventral (C) view. Dashed line boxes indicate the parts of the chondrocranium which are of the mesodermal origin



relatively small concave cartilaginous plate. Medially, it closely approaches the lateral side of the anterior portion of the interorbital septum, but does not fuse with it (Figures 3 and 4). Laterally, the planum antorbitale is fused with the paranasal cartilage. Dorsally, the planum antorbitale bears a cartilaginous process—the paraseptal cartilage, which travels along the ventrolateral edge of the nasal septum. In *A. fragilis*, the paraseptal cartilage is a blindly ending narrow cartilaginous plate. Its ventromedial surface attaches to the dorsolateral surface of the medial part of the vomer (Figures 4B,C and 5B,C). The length of the paraseptal cartilage in *A. fragilis* is

approximately one third of the total length of the nasal capsule. Unlike *A. fragilis*, the paraseptal cartilage in *P. apodus* is fused anteriorly with the lamina transversalis anterior (Figures 3 and 5B,C). The vomerine portion of the paraseptal cartilage in *P. apodus* is also represented as a narrow cartilaginous plate; however, more anteriorly, the paraseptal cartilage turns into a thin rod of cartilage.

The posterolateral part of the nasal capsule is mainly formed by the paranasal cartilage. This cartilage forms a complex concha, which invades the vestibulum of the olfactory organ. Ventrally, it is fused with the

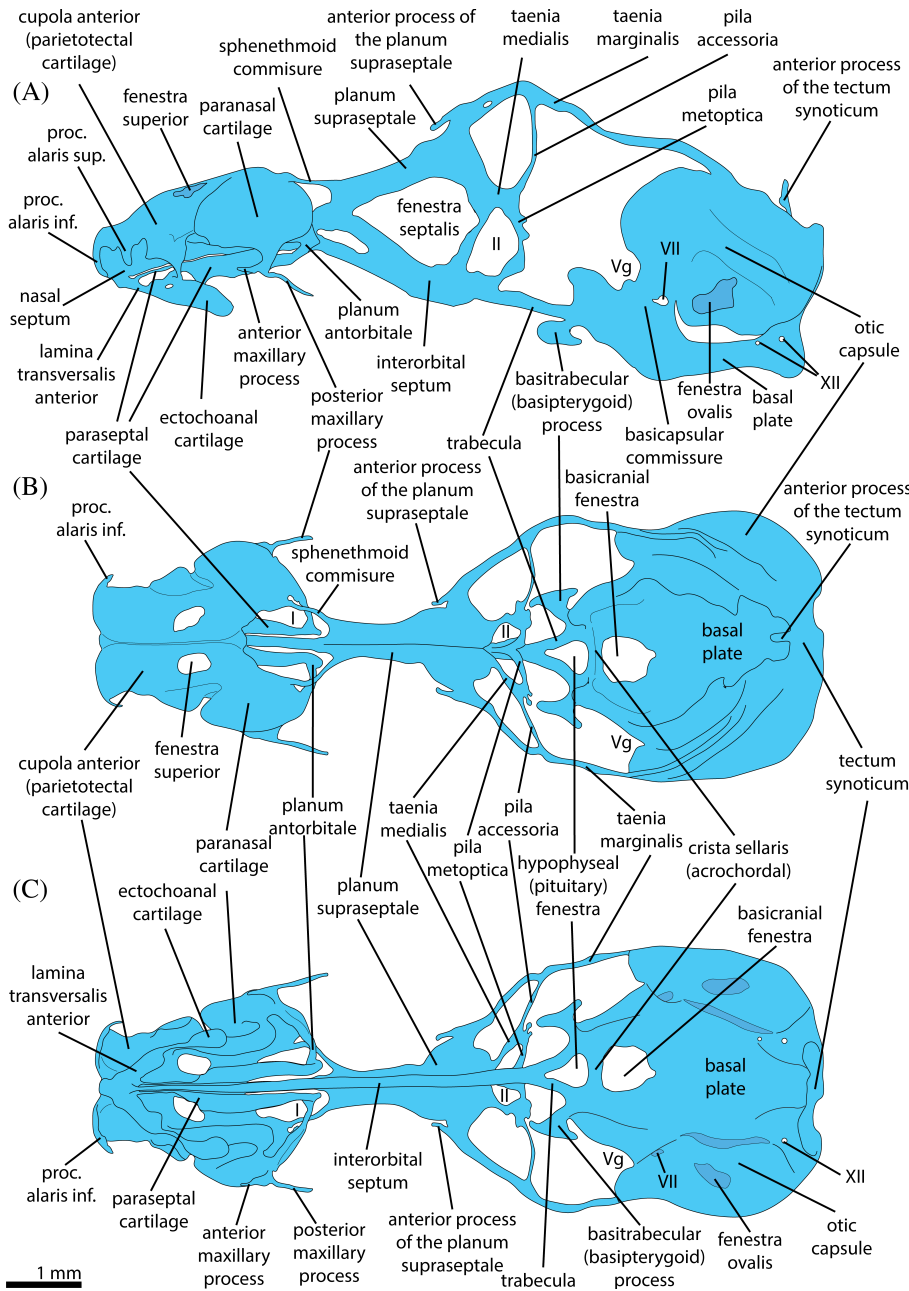


**FIGURE 3** Graphical reconstruction (based on three dimensional reconstruction) of the fully formed chondrocranium of *Pseudopus apodus* in lateral (A), dorsal (B), and ventral (C) view. The pterygoquadrate is not shown here, but the position of the pterygoquadrate in relation to the chondrocranium is shown in Figure 1. Average positions of the olfactory (I) and optic (II) nerves; Vg, trigeminal ganglion; VII and XII, foramina for the facial and hypoglossal nerves, respectively

parietotectal cartilage and posteriorly with the planum antorbitale (Figures 3, 4, and 5C). The ventral part of the paranasal cartilage, which is fused with the planum antorbitale, elongates ventrally and bifurcates in anterior and posterior maxillary processes. Unlike *P. apodus*, these processes are extremely short in *A. fragilis*.

**2.3 | Orbitotemporal region**

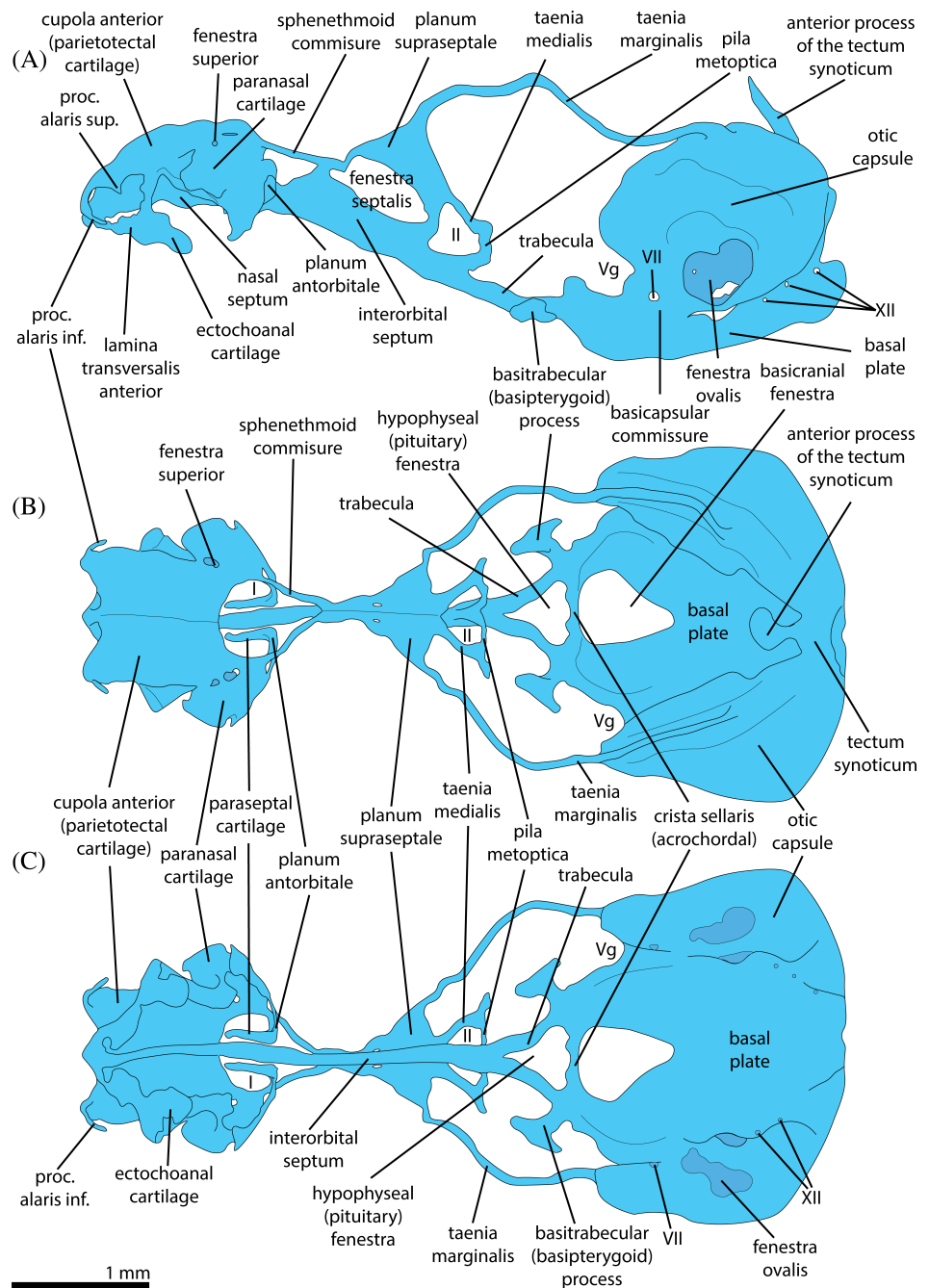
The orbitotemporal region merges into the nasal region. Ventrally, the interorbital septum merges with the nasal septum, and dorsally, the sphenethmoid commissure

connects the planum suprasedale with the parietotectal cartilage surrounding the foramen for the ophthalmic nerve.

In both species, the interorbital septum is high and extremely thinned in its middle portion forming a fenestra, which is filled with a very thin membrane - the fenestra septalis (Figures 3A and 4A). In addition to this, in *Pseudopus apodus*, there is another smaller fenestra, which is also filled with a membrane. It is situated more anteriorly and ventrally to the large fenestra septalis. The anterior border of this small fenestra is approximately on the level of the planum antorbitale.

Dorsally, the interorbital septum bifurcates in a paired cartilaginous plate—the planum suprasedale

**FIGURE 4** Graphical reconstruction (based on 3D reconstruction) of the fully formed chondrocranium of *Anguis fragilis* in lateral (A), dorsal (B), and ventral (C) view. Digits on the figure indicate the position of the respective nerves and ganglion. The pterygoquadrate is not shown here but the position of the pterygoquadrate in relation to the chondrocranium is shown in Figure 2. Average positions of the olfactory (I), and optic (II) nerves; Vg, trigeminal ganglion; VII and XII, foramina for the facial and hypoglossal nerves, respectively



(Figures 3, 4, and 5D), which supports the olfactory tract and partly the anterior part of the telencephalon. It is worth noting that, in *Anguis fragilis*, the anterior part of planum suprasedale abruptly goes down, forming a kink of almost  $90^\circ$  (Figure 4A). Just before this kink, the planum suprasedale is fenestrated by a small oval-shaped foramen, which is not filled with any nerve or blood vessel.

In *P. apodus*, the posterior part of the planum suprasedale bears the anterior process of the planum suprasedale, which is absent in *A. fragilis* (Figures 3A and 5D). The posterodorsal region of the planum suprasedale in both species continues with a taenia

marginalis, the rod-shaped cartilage, whose posterior end reaches the dorsal surface of the otic capsule (Figures 3, 4, and 5E,F). In *P. apodus*, taenia marginalis has a small foramen, just behind the planum suprasedale.

The posteroventral part of the planum suprasedale in both species continues as the taenia medialis. Posteriorly, the taenia medialis is fused with the pila metoptica. The pilae metoptica of both body sides are fused to each other ventrally and are located anteroventrally to the interorbital septum (Figures 3 and 4). Thus, the taenia medialis dorsally, the pila metoptica posteriorly, and the interorbital septum anteriorly restrict the foramen for the

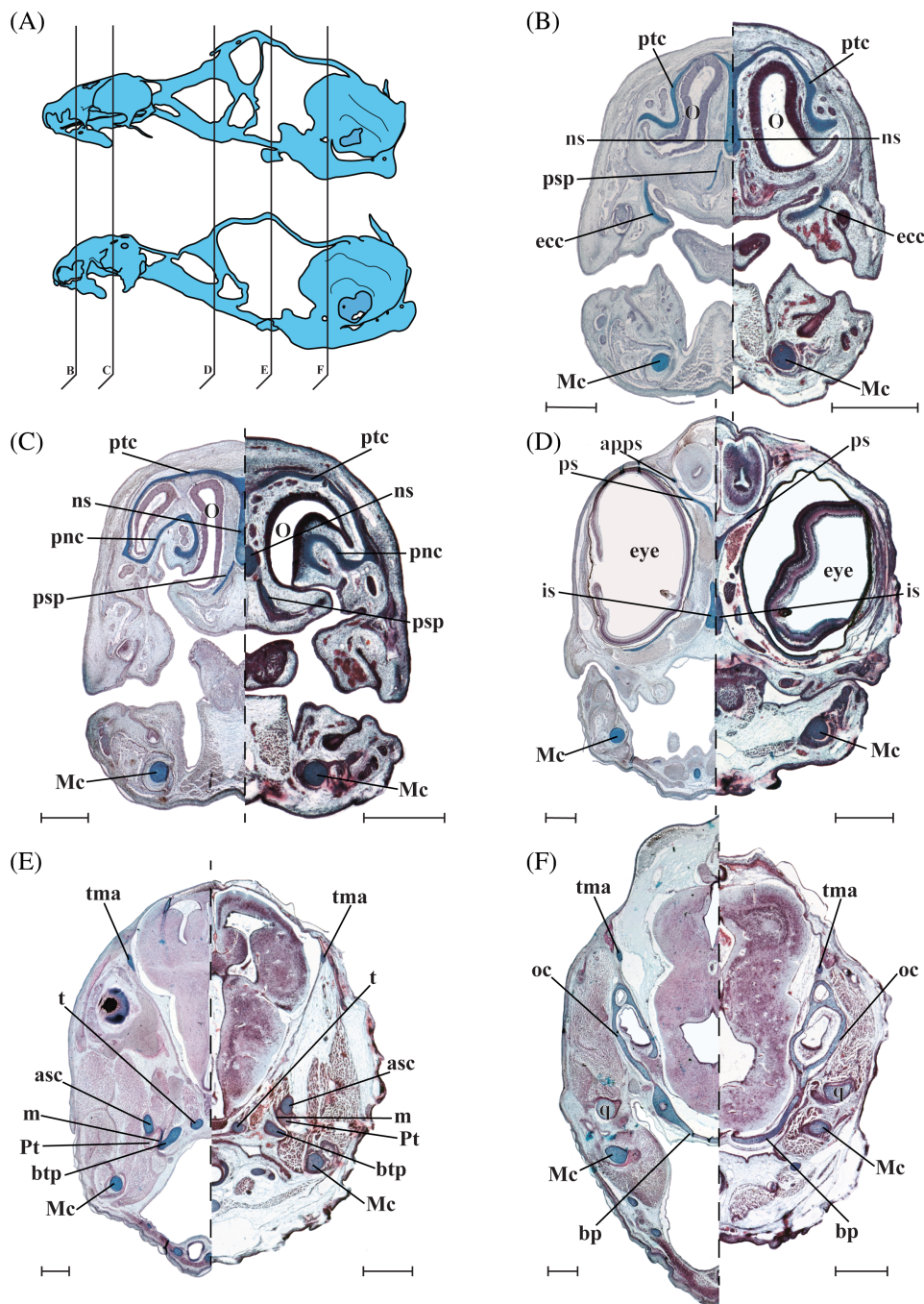


**FIGURE 5** Cross sections (10  $\mu\text{m}$ ) through the embryonic heads of *Pseudopus apodus* (left side) and *Anguis fragilis* (right side) arranged in anterior (B) to posterior (F) order; level of each section is shown on the graphical reconstructions in the lateral view (A). asc, ascending process; apps, ascending process of the planum suprasetale; bp, basal plate; btp, basitrabecular process; ecc, ectochoanal cartilage; is, interorbital septum; m, pterygoid meniscus; Mc, Meckel's cartilage; ns, nasal septum; O, olfactory organ; oc, otic capsule; pnc, paranasal cartilage; ps, planum suprasetale; psp, parasetal cartilage; Pt, pterygoid bone; ptc, parietotectal cartilage; q, quadrate; t, trabeculae; tma, taenia marginalis. Scale bars equal 500  $\mu\text{m}$

optic nerve. In *P. apodus*, this foramen has a trapezoid form, and in *A. fragilis*, this foramen is more triangular (Figures 3A and 4A).

From the fusion point of the taenia medialis and pila metoptica in *P. apodus*, there is another vertical cartilaginous bar—the pila accessoria (Figure 3). Dorsally, it is fused with the taenia marginalis. The pila accessoria is completely absent in *A. fragilis*.

Posterior to the place of fusion with the pila metoptica, the interorbital septum continues with the trabecula communis, which in its turn bifurcates just before the

pituitary into the trabeculae. Posteriorly, the trabeculae are fused with the crista sellaris, and together, they restrict the pituitary fenestra (Figures 3B,C and 4B,C).

In both species, laterally, the place of fusion of the acrochordal and the posterior end of the trabecula on the level of the posterior border of the hypophyseal fenestra and laterally to it branches off the basitrabecular or the basiptyergoid process (Figures 3, 4, and 5E). Through the cartilaginous pad, that is, the basiptyergoid meniscus, the basiptyergoid process articulates with the pterygoid (Figure 4E). In *P. apodus* the basiptyergoid meniscus

completely covers the articulation surface, while in *A. fragilis* the meniscus covers only the anterior part of it (Figures 1 and 2).

The basiptyergoid process goes lateroventrally and is oriented in an anterior direction. It represents a stipe with a footplate (articulating surface) in its distal portion and is reminiscent of a mushroom shape in a dorsal and ventral view. The distal portion of the footplate of the basitrabecular process is dorsoventrally flattened, thus the articulating surface is elliptic in shape. In *P. apodus*, the basiptyergoid process is oriented more ventrally compared to *A. fragilis*.

## 2.4 | Otic capsules and the basal plate

The posterior part of the chondrocranium is represented by the paired otic capsules and the basal plate with the occipital arches posteriorly and parachordals anteriorly. The parachordals are anteriorly fused to the acrochordal or crista sellaris, which ossifies as the “Turkish seat” (sella turcica) in later development.<sup>5,20,23</sup> The parachordals and the acrochordal restrict the basicranial fenestra. In *Anguis fragilis*, the basicranial fenestra is relatively bigger than in *Pseudopus apodus* and more triangular in shape (Figures 3B,C and 4B,C). Along the midline of the basal plate and partly embedded in its dorsal surface lies the cranial portion of the notochord. It goes along the basicranial foramen and reaches the posterior surface of the acrochordal (Figures 1 and 2).

In both species, the otic capsules are roundish and slightly elongated and bear the utricles (Figures 3, 4, and 5F). The lateral wall of the otic capsule bears a big oval foramen (fenestra ovale). It is relatively bigger in *A. fragilis*. Anteromedially, the otic capsule is fused with the dorsolateral aspect of the parachordal by the basicapsular commissure. The basicapsular commissure contains a small foramen for the facial nerve (Figures 1A and 2A). Posteriorly, the otic capsule is fused with the occipital arch. Posterodorsally, both otic capsules are fused by a relatively broad cartilaginous band—the tectum synoticum. It is invaginated posteriorly, and, anteriorly, it bears the anterior process of the tectum synoticum. In *A. fragilis*, it is oriented anterodorsally, whereas it has a more or less strait dorsal orientation in *P. apodus*.

## 2.5 | Palatoquadrate

Palatoquadrate in both species is represented by the ascending process and the quadrate (Figures 1 and 2). The ascending process represents a bar-shaped vertical cartilage with the base placed on the dorsal surface of the

ptyergoid, where the pterygoid articulates with the pterygoid menisc (Figure 5E).

The quadrate in both species can be divided into the mandibular and tympanic portion. The mandibular portion is elongated and flattened, the tympanic portion is bean shaped and its dorsolateral surface bears an additional thin cartilaginous bar, which forms a loop. The major difference between *Pseudopus apodus* and *Anguis fragilis*, is that in *P. apodus* this loop is more prominent (Figures 1 and 2).

## 2.6 | Developmental aspects of the *Pseudopus apodus* chondrocranium

*Stage 1* (Figure 6). In the earliest stage available to us in our sampling, it is already possible to define all chondrocranial structures that are characteristic of the fully formed chondrocranium of this lizard; however, the anterior part of the chondrocranium, namely the nasal region, is mostly represented as a condensation of the mesenchyme. The cartilaginous parts also have uncertain borders as the peripheral areas of the structures still contain a certain amount of the undifferentiated mesenchymal cells. The general axis of the chondrocranium is quite curved and reflects the shape of the brain at this stage (Figure 6).

The crucial difference with the late, that is, tempus optimum, stage described previously (Section 2.1; Figures 1 and 3) is the presence of the pila antotica, which is absent in the later stage (Stage 2). The pila antotica is a thin and weakly chondrified band of tissue, which connects the lateral aspects of the acrochordal with the fusion point of the pila metoptica, taenia medialis, and pila accessoria. The pila metoptica does not fuse with the trabecula ventrally. There is a foramen filled with the mesenchyme in the region of fusion of taenia medialis and the three pilae. Dorsally, the pila accessoria is continuous with the taenia marginalis forming a T-shaped structure (Figure 6). At this stage, the posterior edge of the taenia marginalis reaches the dorsal aspect of the otic capsule but does not fuse with it. The anterior end of the taenia marginalis is situated a short distance from the posterior edge of the planum suprasedptale, but is also not merged with it. A basitrabecular process is present only as a condensation of the mesenchymal cells positioned between the place of fusion of the trabecula and the acrochordal cartilage (crista sellaris) and the base of the ascending process.

A tectum synoticum is absent and there is no fusion between the occipital arch and the otic capsule. Also, the otic capsules are only fused with the basicranium anteriorly.

The palatoquadrate is represented by the ascending process and the quadrate. Both elements are mostly represented as a very dense condensation of the



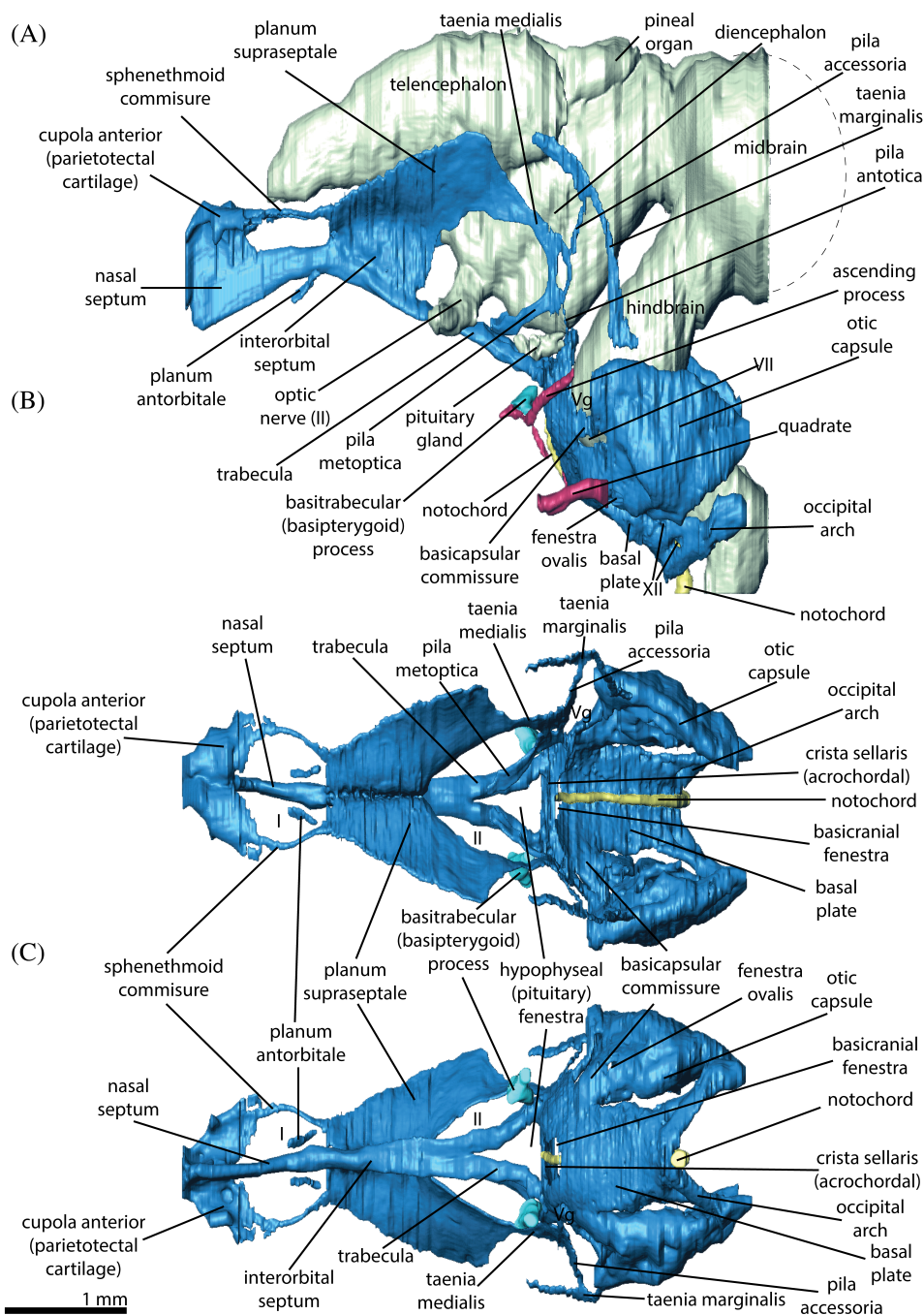


**FIGURE 6** 3D reconstruction of the developing chondrocranium (in blue), brain (in light yellow), and the elements of the palatoquadrate (in purple) of *Pseudopus apodus* at stage 1 in lateral (A), dorsal (B), and ventral (C) view. Average positions of: the olfactory (I), and optic (II) nerves; Vg, trigeminal ganglion; VII and XII, foramina for the facial and hypoglossal nerves, respectively. Due to the few missing terminal histological sections of the head the dashed lines indicate the approximate shape of the organs. At these stages the large part of the chondrocranium in active development, thus, the real borders of the cartilage are uncertain as it also contains a lot of undifferentiated mesenchymal cells especially in the nasal region

mesenchyme with only a few chondrocytes. The base of the ascending process bears two mesenchymal outgrowths, the anterior one representing the pterygoid process and the posterior one oriented toward the quadrate. The quadrate is a bean-shaped structure and, in its base, it also bears a mesenchymal outgrowth oriented toward the posterior outgrowth of the ascending process (Figure 6).

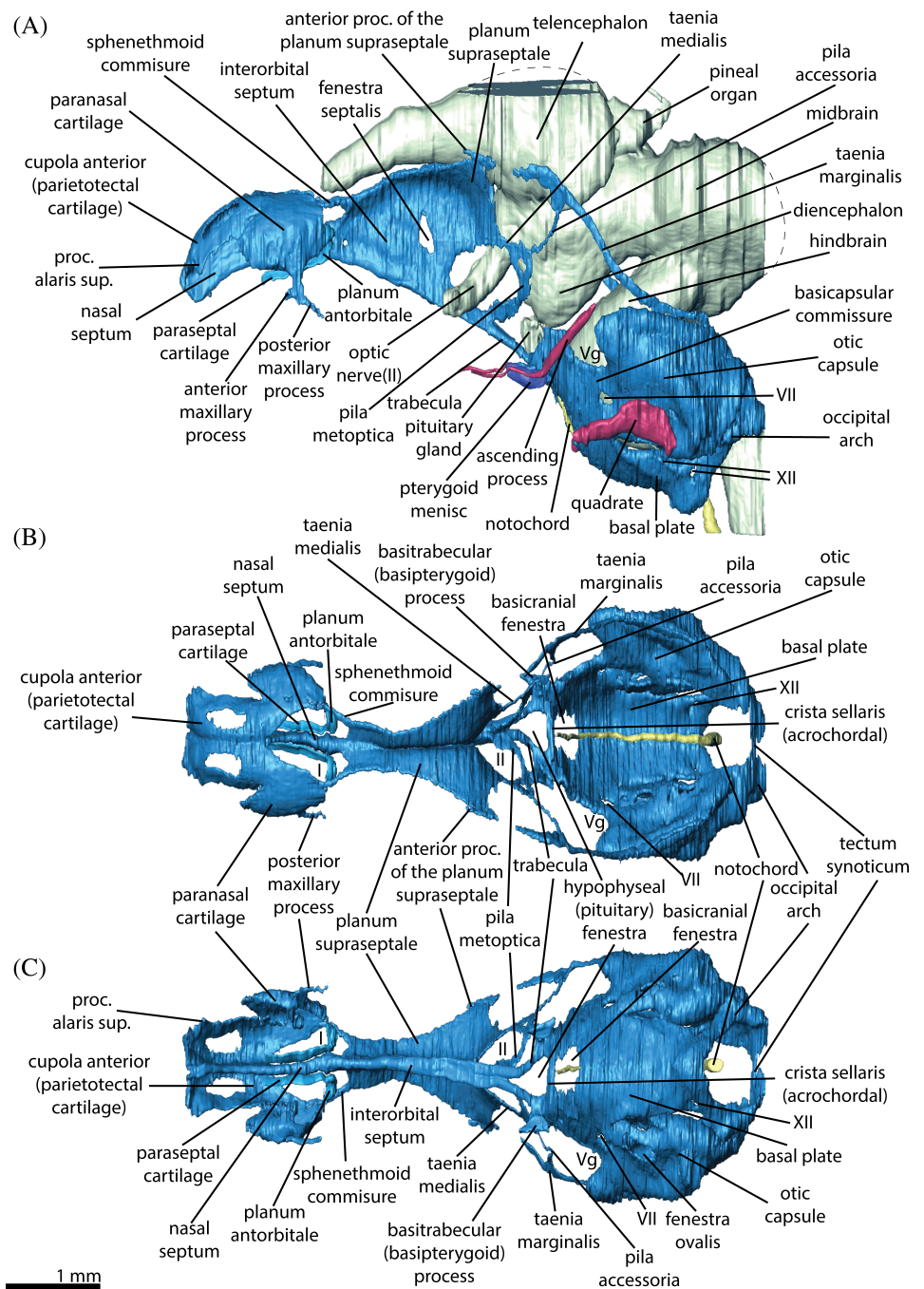
**Stage 2** (Figure 7). In the second developmental stage available to us in our sampling, the chondrocranium almost acquires the shape of the fully formed chondrocranium. The mesencephalic flexure is almost gone. The nasal region undergoes further chondrification and

structural differentiation; however, it is not completely chondrified yet.

The pila antotica is not present anymore, but the place of fusion between the remaining pilae and the taenia medialis still contains a foramen (Figure 7), which is now smaller. The posterior end of the taenia marginalis is already fused with the otic capsule. The anterior part of the taenia marginalis ends freely. It is possible to distinguish a small outgrowth from the posterodorsal edge of the planum suprasedptale, which points toward the anterior portion of the taenia marginalis.

The posterior region of the chondrocranium has already reached the fully formed condition, that is, the otic

**FIGURE 7** 3D reconstruction of the developing chondrocranium (in blue), brain (in light yellow) and the elements of the palatoquadrate (in purple) of *Pseudopus apodus* at stage 2 in lateral (A), dorsal (B), and ventral (C) view. Average positions of: the olfactory (I), and optic (II) nerves; Vg, trigeminal ganglion; VII and XII, foramina for the facial and hypoglossal nerves, respectively. Due to the few missing terminal histological sections of the head the dashed lines indicate the approximate shape of the organs. At these stages the large part of the chondrocranium is in active development, thus, the real borders of the cartilage are uncertain as it also contains a lot of undifferentiated mesenchymal cells especially in the nasal region



capsule is fused posteriorly with the occipital arch. The tectum synoticum is already cartilaginous, however, the anterior process of the tectum synoticum is not yet developed.

### 3 | DISCUSSION

#### 3.1 | Evolution of anguid chondrocranial anatomy

In general, the anatomy and the architecture of the chondrocranium in *Pseudopus apodus* and *Anguis fragilis* are

very similar and comparable both to each other and to those of most other lizards (see Reference 5).

The nasal region in both species contains all elements diagnostic for squamates, namely nasal septum, parietotectal cartilage, paranasal cartilage, planum antorbitale with the paraseptal cartilage, and lamina transversalis anterior. The composition of these structures is also similar to most other lizards. The only principal difference between *P. apodus* and *A. fragilis* is that the paraseptal cartilage in *A. fragilis* does not fuse anteriorly with the lamina transversalis anterior. This feature, however, has also been observed in some other lizard clades<sup>38,39</sup>

and is characteristic of snakes.<sup>5</sup> The developmental pattern of the paraseptal cartilage in *P. apodus* is comparable to the lacertids for example<sup>23</sup>; that is, in all of them the paraseptal cartilage fuses anteriorly with the lamina transversalis anterior. *A. fragilis*, however, retains a paedomorphic state of the paraseptal cartilage when compared to other squamates.

The orbitotemporal region in *P. apodus* and *A. fragilis* is represented by the interorbital septum, planum suprasedale, pila metoptica, taenia marginalis, and taenia medialis. Both species lack the pila antotica in the fully formed chondrocranium. Furthermore, in addition to the pila antotica, the pila accessoria is completely absent in *A. fragilis*. Both pilae are present in *P. apodus* in early ontogeny; however, the pila antotica never completely chondrifies, and late in embryogenesis it undergoes reduction. The ontogenetic regression of the pila antotica which takes place in *P. apodus*, is well documented for other clades of lizards, like gymnophthalmids,<sup>40</sup> skinks,<sup>17,19,41,42</sup> varanids,<sup>43</sup> agamids,<sup>39,44,45</sup> and chamaeleonids,<sup>46,47</sup> too. By

extrapolating the developmental traits of the pila accessoria of lacertid lizards<sup>23-26,48,49</sup> to *A. fragilis*, the absence of the pila accessoria in the fully formed chondrocranium suggests a complete absence of the pila antotica in this species early in ontogeny.<sup>6,20</sup> The anatomy of the orbitotemporal region in *A. fragilis* closely resembles that of gekkonid lizards, in which pila antotica and pila accessoria are also completely absent<sup>10-12,50-52</sup> (Figure 8).

### 3.2 | Development of the chondrocranium and dual origin of taenia marginalis in anguids

By tracing the development of the chondrocranium in *Pseudopus apodus*, we can state that the general pattern of its development is similar to that of most other vertebrates. The chondrification of the skull proceeds from posterior to anterior, that is to say the nasal region is last to chondrify.<sup>23,53-55</sup>

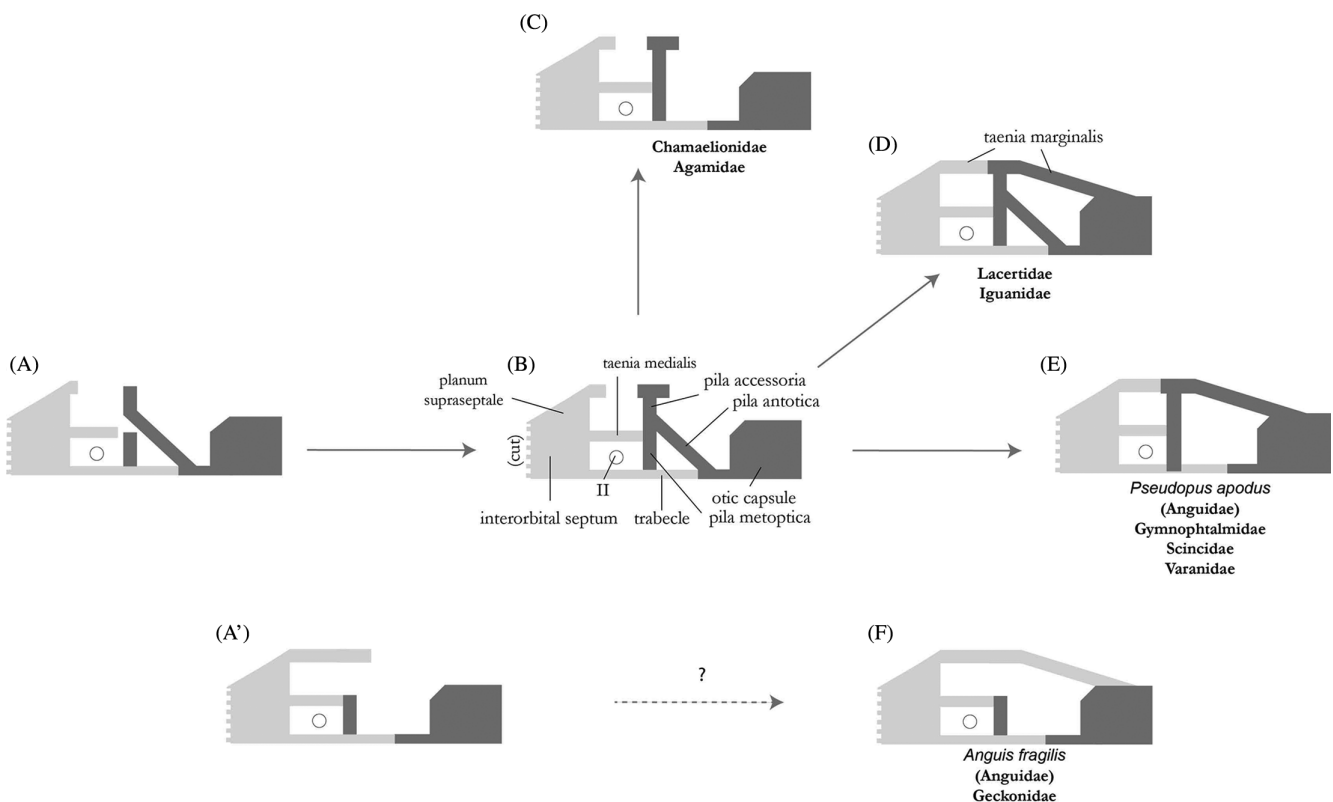


**FIGURE 8** Evolution and development of the orbitotemporal region in major lizard clades; schematic illustrations (in lateral view) of developmental models (A, A', B) and the diversity (C-F) and of the chondrocrania. Structures of neural crest and mesodermal origin are in light and dark grey, respectively. Developmental model A/B is based on lacertid lizard data.<sup>23</sup> B/E correspond to the fully formed chondrocrania in scincids,<sup>18,19,42</sup> varanids,<sup>43</sup> gymnophthalmids,<sup>40</sup> and *Pseudopus apodus*, that is, clades of lizards in which pila antotica undergoes ontogenetic regression. Developmental state shown in B also corresponds to chamaeleonids.<sup>38,46</sup> C corresponds to the fully formed chondrocrania in chamaeleonids and agamids,<sup>38,39</sup> and D to lacertids<sup>23,25,59</sup> and iguanids.<sup>92</sup> A' illustrates the hypothetical developmental model for *Anguis fragilis*, where taenia marginalis develops completely from planum suprasedale. F corresponds to gekkonids<sup>10,11,50-52</sup> and to *A. fragilis* described herein

Although we did not have access to the earliest developmental stages of the anguids, the existing data helps to interpret the diversification of the orbitotemporal region in squamates. As we already pointed out above, pila antotica in *P. apodus* is present only in the early developmental stage; its upper part, however—the pila accessoria—remains at the later stage, but is not present in *Anguis fragilis*. Based on the developmental sequence of *P. apodus*, the pila accessoria gives rise to the largest part of the taenia marginalis. It is only at the late stage that the latter fuses with the anterior portion of the taenia marginalis, which grows from the planum suprasedale. A similar developmental pattern can be observed in other squamates.<sup>23,25</sup> Remarkably, despite the absence of the pila accessoria in *A. fragilis*, the taenia marginalis is well developed in this species and connects the planum suprasedale with the otic capsule. The presence of the taenia marginalis without the presence of the pila accessoria is characteristic also to some other clades of squamates, including geckos<sup>12,50</sup> and *Anniella pulchra*.<sup>56</sup> The latter belongs to Anniellidae, which, together with Anguillidae, form a sister clade to Varanidae.<sup>28</sup>

In the skull of vertebrates, the trabeculae are of neural crest origin and the acrochordal cartilage is of premandibular mesoderm origin.<sup>57,58</sup> Thus, the derivatives of the trabeculae (namely interorbital septum and planum suprasedale), and the derivatives of the acrochordal cartilage (namely the pila antotica and the pila accessoria), might, respectively, be of neural crest and mesodermal origin as well.<sup>20</sup> Given the probability that no other, local cells are recruited for the formation of the taenia marginalis and that the taenia marginalis is indeed an outgrowth of the pila accessoria (further study of intermediate developmental stages would be needed to prove this), we hypothesize that the taenia marginalis in *P. apodus* and *A. fragilis* are not homologous to each other. In other words, when the taenia marginalis develops directly from the planum suprasedale, it might be of neural crest origin, whereas when it develops mostly from the derivatives of the acrochordal, it might be of mesodermal origin. Concerning the later fusion of the taenia marginalis with the bar-like posterodorsal outgrowth of the planum suprasedale in *P. apodus*, its taenia marginalis would be of double origin.

### 3.3 | Evolutionary and ontogenetic simplification of the orbitotemporal region

In spite of the fact that the chondrocrania of both species are very similar in their general architecture, the specifications—especially of the overall shape and the shape of particular structures—are surprisingly different.

Lacertid lizards, however, show a different condition: the fully formed chondrocrania look very similar among different species and only some minor proportional differences exist.<sup>23,25,59-61</sup> The heterochronic shifts in the development of particular structures might correlate to ecological adaptations but do not affect the general anatomy of the chondrocrania in this clade.<sup>23,62</sup> One may assume that the great variability of the chondrocrania in closely related species of anguillids could be explained by the time of evolutionary divergence between species; however, the divergence time between *Anguis* and *Pseudopus* is much shorter (median time 14.4 MYA) compared to the time of divergence between closely related species of the genus *Lacerta* (median time 21.7 MYA).<sup>63</sup>

Considering that the chondrocrania in reptiles are inherited from early vertebrates, they might retain a very conservative pattern of their general structure.<sup>3,6</sup> However, in different lepidosaur clades, simultaneous complications and simplifications of chondrocranial structures can be observed (Figure 9). Evolution of the olfactory sense, that is, the elaboration of the vomeronasal and the olfactory organ, required modifications of the nasal capsule by forming an additional concha. This can be easily detected when comparing the structures of the nasal capsules between archelosaurians (ie, turtles, crocodiles, and birds<sup>64</sup>) and lepidosaurs (ie, *Sphenodon punctatus* and squamates). The opposite situation can be observed in the orbitotemporal region of the chondrocranium, which is well formed in the Archelosauria, but becomes more gracile in *S. punctatus* and tends to be reduced in squamates.<sup>5,6,8,65-72</sup>

### 3.4 | Correlation of the reduction of the chondrocranium and the limbs

The observation of the squamates' chondrocranial anatomy indicates that reduction in the orbitotemporal region somehow correlates with different types of limb reduction, body elongation, and clearly with skull kinesis. For instance, snakes hold the most extreme position in this regard, with an almost completely reduced orbitotemporal region of the chondrocranium (with rare cases of unfused orbital cartilages present<sup>73</sup>). Nevertheless, the reduction of the snake chondrocranium is very different in comparison to lizards and is reflected in a platitric condition of the chondrocranium. In snakes, trabeculae never fuse in the orbital region and formation of the interorbital septum and its derivatives becomes impossible.<sup>5</sup> In turn, the reduction of the orbitotemporal region in lizards mostly affects the pilae and taeniae, sometimes the interorbital septum,<sup>72,74</sup> but never the trabeculae. From known evidence, only a few lizards

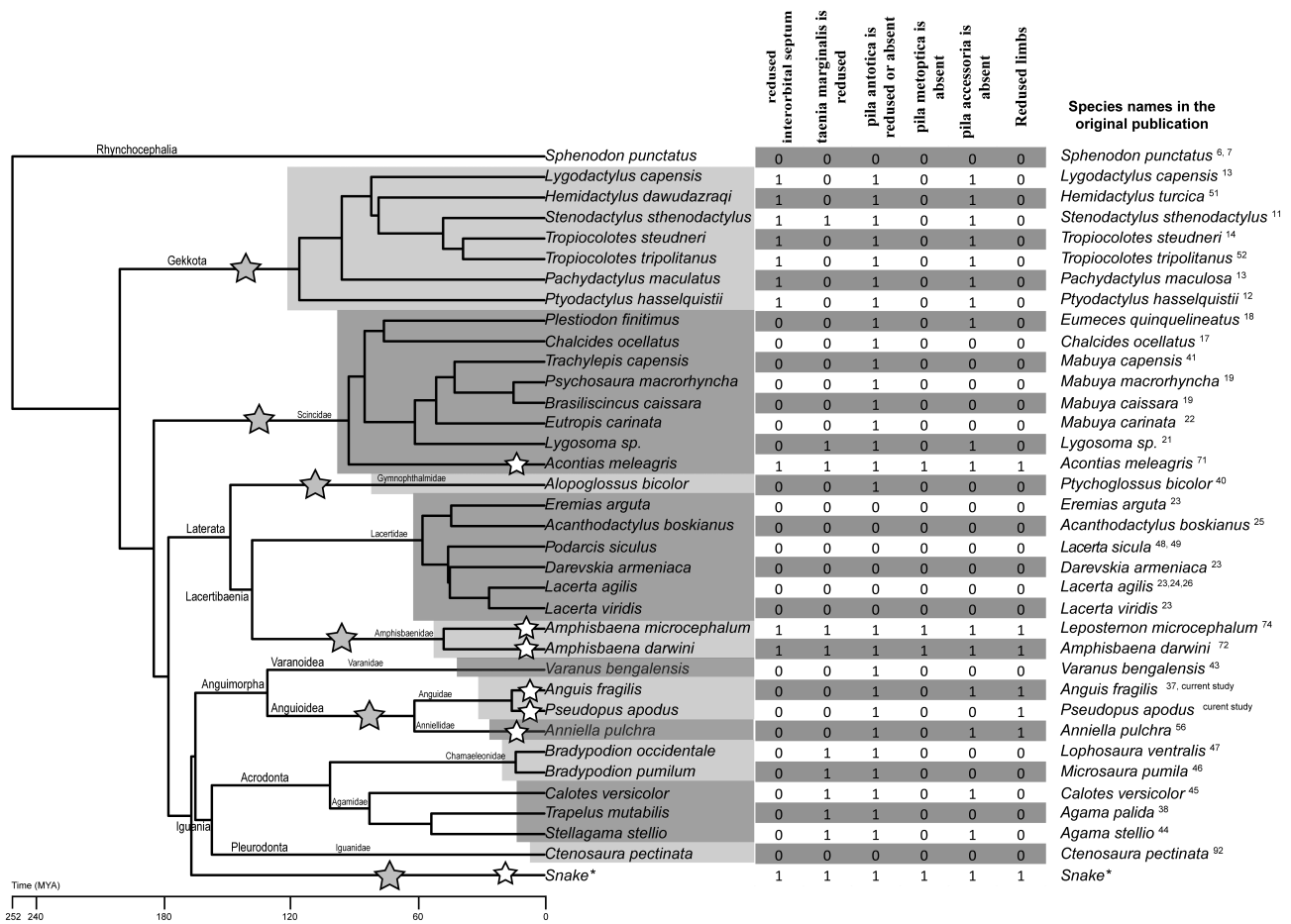


**FIGURE 9** Phylogenetic tree (time scaled) of lepidosaur reptiles after Zheng & Wiens (2016) with the table of the anatomical features which were used for the correlation test. Only species with the known chondrocranial anatomy are included. Gray asterisks indicate the clades with known limbless representatives. White stars indicate limbless species in the current dataset

possess an almost similar condition to the snake's trait, where the orbitotemporal part of the chondrocranium is almost completely missing. This can be found in *Amphisbaenia*<sup>72,74</sup> and *Scincidae*.<sup>71</sup> In addition, there is a complete absence of limbs in these lizards.

High variability of the chondrocranial anatomy in the orbitotemporal region in closely related species of anguids suggests that there might be correlation between the grade of chondrocranium reduction and limb reduction, which is also highly variable on lower taxonomic level. To evaluate this hypothesis, we have summarized available data on the chondrocranial and body anatomy (Figure 9) of lepidosaurs. In order to avoid overloading the dataset with the squamate species with high grade chondrocranium and limb reduction, we only included one snake species.

The available dataset of species demonstrates a significant correlation between extreme reduction in chondrocranium and extreme reduction in limbs. The extreme reduction in chondrocranium is defined as a state in which all five considered components of the chondrocranium are reduced or missing. The extreme reduction of

**TABLE 1** Statistics of extreme reduction in chondrocranium and limbs among species for which chondrocranium was assessed

Number of species with:	Extreme reduction in the chondrocranium	No extreme reduction in the chondrocranium
Extreme reduction in the limbs	4	3
No extreme reduction in the limbs	0	29

limbs is defined as a morphology, in which limbs are not visible. Out of the 36 species considered, four have extreme reductions in both chondrocranium and limbs, three more have extreme reduction in limbs but not in chondrocranium, while the remaining 29 species have no extreme reductions; no species features extreme reduction in limbs but not in the chondrocranium (see Table 1). The Pearson correlation coefficient between extreme reductions is about 0.72. The Pearson correlation

coefficient is defined as the ratio of covariance between two variables to the product of their standard deviations. For our data set it is

$$\rho = \frac{4 \cdot 29 - 3 \cdot 0}{\sqrt{(4+0)(3+29)(4+3)(29+0)}} \approx 0.72$$

However, the dataset is not large and the classes of extreme reductions are not balanced; the majority of the dataset comprises species without extreme reductions. Hence, to confirm that the suggested association between extreme reductions in chondrocranium and limbs is statistically significant, we also considered the null hypothesis that these reductions appear randomly and independently of each other. For that, in a random dataset, we kept the size of the experimental sample and preserved the observed balance of classes: so, there are 36 species, seven of them have extreme reduction in limbs, and four species have extreme reduction in chondrocranium. In the null model, however, these extreme reductions may appear in different species. We found that the observed correlation value of 0.72 is the largest value that can ever be obtained among all possible configurations. According to the null hypothesis, which assumes that the extreme reductions in chondrocranium and limbs are independent and not-correlated, the probability that all limbless species will also have an extreme reduction in chondrocranium is only about 0.00059 (see Supporting Information S1 for details). Therefore, we conclude that it is highly unlikely that the absence of correlations stated in null hypothesis is true.

### 3.5 | Possible genetic links between the reduction of the chondrocranium and the limbs

One possible explanation of such a strong correlation might be hidden in developmental genetic mechanisms of body elongation and limb rudimentation. We assume, that the pleiotropic effect<sup>75</sup> of particular genes which affect the chondrocranium development in squamates could also be reflected in the body elongation and limb loss. Potentially, this can explain the diversity of the chondrocranial anatomy in the clades in which representatives with different grades of the limb reduction and body elongation are present, as has been shown in the current study. This hypothesis clearly requires further research, but apparently, the genetic mutations which enabled to evolve serpentiform bodies also caused various differences in chondrocranium rudimentation in squamates.

Evidence from mammalian embryology supports the idea that genetic mechanisms underlying limb malformation in most cases also effect malformations of the skull.<sup>76</sup> Recent studies on model organisms indicate that numerous molecules involved in craniofacial morphogenesis have a pleiotropic effect and also serve as inducing or patterning signals during the development of the limbs. The knockdown experiments of single genes performed in mouse embryos, together with evidence from several congenital human syndromes, have shown<sup>77-80</sup> that craniofacial anomalies are often accompanied by diverse limb malformations. For instance, deregulation of BMP (bone morphogenetic protein) signaling has a wide range of effects on the formation of chondrocranium and skull as a whole<sup>81</sup> and at the same time it is a part of self-regulatory limb bud signaling.<sup>82</sup>

As another example, *Shh* (Sonic hedgehog) reportedly has a key function in both craniofacial and limb formation. It has been shown that *Shh* is emitted from distinct sources at specific developmental time-points and is responsible for the proper and independent formation of structures such as the posterior part of the nasal capsule, the nasal roof, and the nasal septum.<sup>55,83</sup> It is useful to note that a function of genomic regulatory regions was shown to be responsible for affecting the levels of *Shh* in various regions, resulting in surprisingly diverse effects on the anatomy and morphometrical features of chondrocranial parts.<sup>55</sup> This mechanism may be the evolutionary basis for the diversity of chondrocranial shapes in vertebrates.

The vertebrate skull originates from two main sources of cells<sup>84</sup>: of mesodermal and of the neural crest origin (Figure 8). It is worth noting that *Shh* gene has a pleiotropic effect on both derivatives of the neural crest (nose region, which largely derives from the trabeculae) and of the mesodermal origin (limbs, but not the head mesoderm). In case of most lizards (with the exception of amphisbaenians and geckos, in which both mesodermal and neural crest parts of the chondrocranium are reduced), the reduction of the chondrocranium appears mainly in the structures of mesodermal origin (Figure 9), namely the acrochordal derivatives which make up the great diversity of the orbitotemporal region in squamates, including the pila antotica, the pila accessoria, and (parts of) the taenia marginalis (for more details see Reference 6).

In the current understanding of skull origin,<sup>85-88</sup> the posterior, mesodermal part of the skull is derived from vertebrae, which evolved into the skull base. This important remark leads us to the idea, that the *Hox* (homeobox) genes, which contribute to the trunk segmentation and vertebral column regionalization,<sup>89,90</sup> might be important candidates for testing the hypothesis of a

genetic link between the skull reduction and the body elongation at least in lizards. It might be possible that a mutation involving changes in expression pattern of *Hox* genes affects the regionalization and elongation of the trunk and also has a pleiotropic effect on the head mesoderm resulting chondrocranium rudimentation. It is worth noting that lizards from the clades with limbless representatives usually have missing elements in the orbitotemporal region. This mainly concerns the pila antotica. This phenomenon is possibly an indicator for the evolution of body elongation; however, this is only a speculative idea which also needs to be tested.

It remains unclear what induced the rudimentation of the snake chondrocranium, which lacks both trabecular (neural crest) and acrochordal (mesodermal) derivatives. Likely, the reduction in ancestral snakes initially took place in the chondrocranial structures of mesodermal origin. However, the pedomorphic condition of the trabeculae, that is, the unfused trabeculae in the orbital and orbitotemporal region, suggests that the “original” sequence of developmental events might have been interrupted before the acrochordal derivatives appeared in ontogeny.

## 4 | CONCLUSIONS

In the current study, we present for the first time the morphological description of the fully formed chondrocranium of *Pseudopus apodus* and reanalyzed chondrocranial anatomy of the closely related anguid lizard *Anguis fragilis*. Our observation of the chondrocranium of *A. fragilis* largely agrees with the previous description provided by Zimmermann.<sup>37</sup> The major differences are related to the proportions and shapes of particular regions, which might be related to artifacts in the reconstructions. However, studies on the development of the orbitotemporal region in *A. fragilis* are urgently needed to better understand the nature of the diversification of the orbitotemporal region in squamates.

The fully formed chondrocrania of both species have surprising differences, unusual to find in such closely related species. Besides the differences in the general shape of the chondrocrania, the absence of the pila accessoria and the lack of connection between the parasagittal cartilage and lamina transversalis anterior in *A. fragilis* is the most intriguing.

The Pearson correlation coefficient indicates strong correlation between reductions in chondrocrania and limbs. Though purely speculative, we consider for future studies the possibility that changes in the chondrocranial anatomy of squamates might be linked to the evolution of limblessness by means of genetic mechanisms.

## 5 | EXPERIMENTAL PROCEDURES

### 5.1 | Embryonic material

The embryonic material of *Pseudopus apodus* was obtained from one gravid female, which was captured in its natural habitat on the Balkan peninsula (Black Mountains) in 2001. The eggs were laid on May 22nd, 2001; the first embryo was dissected on June sixth (Stage 1), the hatching took place (Stage 7) on July 20th. The seven eggs were successfully incubated on a moist substrate at 26 to 28°C. The humidity was 91% to 96%. The *Anguis fragilis* embryos were obtained from gravid females collected from their natural habitats in Eastern Slovakia (Eastern Carpathians) in 2001, and bred in the collections of the Department of Ecology, Comenius University in Bratislava, Faculty of Natural Sciences.

For the current study, for both species, we concentrated on a stage with a fully formed chondrocranium that corresponds to the “tempus optimum” criteria<sup>54</sup> (*A. fragilis*—š9, *P. apodus*—š5) plus two earlier stages in *P. apodus* (š2 and š3) to trace the development of particular structures in the orbitotemporal region.

### 5.2 | Histological data

The embryonic material of both species was embedded in paraffin and serially sectioned with a rotary microtome at 10 µm slide thickness. After sectioning, the histological slides were stained with erythrosine and Mayer's hematoxylin and, to determine cartilage, with Alcian blue.<sup>91</sup>

The histological sections are stored in Comenius University in Bratislava, Faculty of Natural Sciences, Department of Ecology (Slovakia).

### 5.3 | Image processing

The histological sections of both species were photographed using an Olympus BH-2 microscope equipped with the Sony α7 digital camera. Using the Avizo 8.1. software package (Thermo Fisher Scientific), the images were aligned using the semiautomatic function, and the manual segmentation tool was applied to create 3D reconstructions of the chondrocrania. Based on the original 3D models, the schematic drawings of the chondrocrania were prepared using Adobe CC software package.

## ACKNOWLEDGMENTS


The authors are grateful to Michael W. Caldwell and one anonymous reviewer for their valuable suggestions. This

study was supported by the Scientific Grant Agency of Ministry of Education of Slovak Republic and Slovak Academy of Sciences, Grant Number 1/0228/19 granted to J.K. and by DFG-funds WE 5440/5-1 and WE 5440/6-1 granted to I.W.

## AUTHOR CONTRIBUTIONS

**Oleksandr Yaryhin:** Conceptualization; investigation; supervision; visualization; writing-original draft. **Ingmar Werneburg:** Conceptualization; resources; supervision; writing-original draft. **Josef Klembara:** Data curation; methodology; writing-original draft. **Marketa Kaucka-Petersen:** Writing-original draft. **Yuriy Pichugin:** Formal analysis; methodology; writing-original draft.

## ORCID

Oleksandr Yaryhin  <https://orcid.org/0000-0003-0363-2057>

Jozef Klembara  <https://orcid.org/0000-0001-8969-3488>

Yuriy Pichugin  <https://orcid.org/0000-0003-3078-2499>

Marketa Kaucka  <https://orcid.org/0000-0002-8781-9769>

Ingmar Werneburg  <https://orcid.org/0000-0003-1359-2036>

## REFERENCES

- Jones MEH, Groning F, Dutel H, Sharp A, Fagan MJ, Evans SE. The biomechanical role of the chondrocranium and sutures in a lizard cranium. *J Royal Soc Interface*. 2017;14(137):1-13. <https://doi.org/10.1098/rsif.2017.0637>.
- Kuratani S, Oisi Y, Ota KG. Evolution of the vertebrate cranium: viewed from hagfish developmental studies. *Zoolog Sci*. 2016;33(3):229-238. <https://doi.org/10.2108/zs150187>.
- Werneburg I. Morphofunctional categories and ontogenetic origin of temporal skull openings in amniotes. *Front Earth Sci*. 2019;7:1-7. <https://doi.org/10.3389/feart.2019.00013>.
- Hanken J, Hall BK, eds. The Skull. *Development*. Vol 1-3. Chicago: University of Chicago Press; 1993:587.
- Bellairs AA, Kamal AM. The Chondrocranium and the Development of the Skull in Recent Reptiles. In: Gans CPTS, ed. *Biology of Reptilia*. Vol 11. New York: Academic Press; 1981:1-283.
- Yaryhin O, Werneburg I. The origin of orbitotemporal diversity in lepidosaurs: insights from tuatara chondrocranial anatomy. *Vertebr Zool*. 2019;69(2):169-181. <https://doi.org/10.26049/VZ69-2-2019-04>.
- Schauinsland H. Weitere Beiträge zur Entwicklungsgeschichte der Hatteria. Skelettsystem, schalleitender Apparat, Hirnnerven etc. *Archiv für Mikroskopische Anatomie*. 1900;56(4):747-867.
- Werner G. Das Cranium der Brückenechse, *Sphenodon punctatus* Gray, von 58 mm Gesamtlänge. *Z Anat Entwicklungsgesch*. 1962;123(4):323-368.
- Howes GB, Swinnerton HH. On the development of the skeleton of the tuatara, *Sphenodon punctatus*; with remarks on the egg, on the hatching, and on the hatched young. *Trans Zool Soc London*. 1901;16(1):1-84. <https://doi.org/10.1111/j.1096-3642.1901.tb00026.x>.
- Kamal AM. Observations on the chondrocranium of *Tarentola mauritanica*. *Proc Egypt Acad Sci*. 1965;19:1-9.
- Kamal AM. The chondrocranium of the gecko *Stenodactylus sthenodactylus*. *Proc Egypt Acad Sci*. 1964;18:59-69.
- El-Toubi MR, Kamal AM. The development of the skull of *Ptyodactylus hasselquistii*. II. The fully formed chondrocranium. *J Morphol*. 1961;108:165-191. <https://doi.org/10.1002/jmor.1051080204>.
- Brock GT. Some developmental stages in the skulls of the geckos, *Lygodactylus capensis* and *Pachydactylus maculosa*, and their bearing on certain important problems in lacertilian craniology. *S Afr J Sci*. 1932;29:508-532.
- Kamal AM. Notes on the chondrocranium of the gecko, *Tropicolotes steudneri*. *Bull Zool Soc Egypt*. 1964;19:73-83.
- Kamal AM. The development and morphology of the chondrocranium of *Chalcides* species. *Proc Egypt Acad Sci*. 1969;22:37-48.
- Kamal AM. The fully formed chondrocranium of *Eumeces schneideri*. *Proc Egypt Acad Sci*. 1965;19:13-20.
- El-Toubi MR, Kamal AM. The development of the skull of *Chalcides ocellatus*. II. The fully formed chondrocranium and the osteocranium of a late embryo. *J Morphol*. 1959;105:55-104. <https://doi.org/10.1002/jmor.1051050104>.
- Rice EL. The development of the skull in the skink, *Eumeces quinquelineatus* L. I the chondrocranium. *J Morphol*. 1920;34(1):118-243. <https://doi.org/10.1002/jmor.1050340104>.
- Jerez A, Sánchez-Martínez PM, Guerra-Fuentes RA. Embryonic skull development in the neotropical viviparous skink *Mabuya* (Squamata: Scincidae). *Acta Zool Mexicana*. 2015;31(3):391-402.
- Yaryhin O, Werneburg I. Chondrification and character identification in the skull exemplified for the basicranial anatomy of early squamate embryos. *J Exp Zool Part B*. 2017;328(5):476-488. <https://doi.org/10.1002/jez.b.22747>.
- Pearson HS. The skull and some related structures of a late embryo of *Lygosoma*. *J Anat*. 1921;56(Pt 1):20-43.
- Rao MKM, Ramaswami LS. The fully formed chondrocranium of *Mabuya* with an account of the adult osteocranium. *Acta Zool*. 1952;33(3):209-275. <https://doi.org/10.1111/j.1463-6395.1952.tb00365.x>.
- Yaryhin O, Werneburg I. Tracing the developmental origin of a lizard skull: Chondrocranial architecture, heterochrony, and variation in lacertids. *J Morphol*. 2018;279(8):1058-1087. <https://doi.org/10.1002/jmor.20832>.
- Gaupp E. Das Chondrocranium von *Lacerta agilis*. *Anatomische Hefte*. 1900;14(3):434-594. <https://doi.org/10.1007/bf02296320>.
- Kamal AM, Abdeen AM. Development of chondrocranium of lacertid lizard, *Acanthodactylus boskiana*. *J Morphol*. 1972;137(3):289-333. <https://doi.org/10.1002/jmor.1051370304>.
- de Beer GR. The early development of the chondrocranium of the lizard. *Quarter J Microscopical Sci*. 1930;s2-73(292):707-739.
- Uetz P, Freed P, Hošek J. (eds.) The Reptile Database; 2020 The Reptile Database, <http://www.reptile-database.org>, accessed June 2020.
- Zheng Y, Wiens JJ. Combining phylogenomic and supermatrix approaches, and a time-calibrated phylogeny for squamate reptiles (lizards and snakes) based on 52 genes and 4162 species. *Mol Phylogenet Evol*. 2016;94(Pt B):537-547. <https://doi.org/10.1016/j.ympev.2015.10.009>.
- Werneburg I, Sánchez-Villagra MR. Skeletal heterochrony is associated with the anatomical specializations of snakes among squamate reptiles. *Evolution*. 2015;69(1):254-263. <https://doi.org/10.1111/evo.12559>.



30. Klembara J, Dobiasova K, Hain M, Yaryhin O. Skull anatomy and ontogeny of legless lizard *Pseudopus apodus* (Pallas, 1775): Heterochronic influences on form. *Anat Rec.* 2017;300(3):460-502. <https://doi.org/10.1002/ar.23532>.
31. Klembara J. New finds of anguines (Squamata, Anguinae) from the early Miocene of Northwest Bohemia (Czech Republic). *Palaeontol Z.* 2015;89(2):171-195. <https://doi.org/10.1007/s12542-014-0226-4>.
32. Klembara J, Hain M, Dobiasova K. Comparative anatomy of the lower jaw and dentition of *Pseudopus apodus* and the interrelationships of species of subfamily Anguinae (Anguimorpha, Anguinae). *Anat Rec.* 2014;297(3):516-544. <https://doi.org/10.1002/ar.22854>.
33. Klembara J. A new species of *Pseudopus* (Squamata, Anguinae) from the early Miocene of Northwest Bohemia (Czech Republic). *J Vertebr Paleontol.* 2012;32(4):854-866. <https://doi.org/10.1080/02724634.2012.670177>.
34. Klembara J, Böhme M, Rummel M. Revision of the anguine lizard *Pseudopus Laurillardii* (Squamata, Anguinae) from the Miocene of Europe, with comments on paleoecology. *J Paleo.* 2010;84(2):159-196.
35. Hoffstetter P, Gasc J. *Vertebrae and Ribs of Modern Reptiles. Biology of the Reptilia.* Vol 1. New York: Academic Press; 1969: 201-310.
36. Čerňanský A, Yaryhin O, Ciceková J, Werneburg I, Hain M, Klembara J. Vertebral comparative anatomy and morphological differences in anguine lizards with a special reference to *Pseudopus apodus*. *Anat Rec.* 2019;302(2):232-257. <https://doi.org/10.1002/ar.23944>.
37. Zimmermann. Das Chondrocranium von *Anguis fragilis*. *Anat Anzeiger.* 1913;44:594-606. <https://www.biodiversitylibrary.org/item/43338#page/6/mode/1up>.
38. Zada S. The fully formed chondrocranium of the agamid lizard, *Agama pallida*. *J Morphol.* 1981;170(1):43-54. <https://doi.org/10.1002/jmor.1051700104>.
39. Kamal AM, Zada SK. The early developmental stages of the chondrocranium of *Agama pallida*. *Acta Morphol Neerl Scand.* 1973;11(1):75-104.
40. Hernandez-Jaimes C, Jerez A, Ramirez-Pinilla MP. Embryonic development of the skull of the Andean lizard *Ptychoglossus bicolor* (Squamata, Gymnophthalmidae). *J Anat.* 2012;221(4): 285-302. <https://doi.org/10.1111/j.1469-7580.2012.01549.x>.
41. Skinner MM. Ontogeny and adult morphology of the skull of the south African skink, *Mabuya capensis* (Gray). *Ann Univ Stellenbosch.* 1973;48A(5):1-116.
42. El-Toubi MR, Kamal AM. The development of the skull of *Chalcides ocellatus*. I. The development of the chondrocranium. *J Morphol.* 1959;104:269-306. <https://doi.org/10.1002/jmor.1051040205>.
43. Shrivastava RK. The structure and development of the chondrocranium of *Varanus*. II. The development of the orbito-temporal region. *J Morphol.* 1964;115(1):97-107. <https://doi.org/10.1002/jmor.1051150107>.
44. Eyal-Giladi H. The development of the chondrocranium of *Agama stellio*. *Acta Zoologica.* 1964;45(1-2):139-165. <https://doi.org/10.1111/j.1463-6395.1964.tb00716.x>.
45. Ramasvami LS. The Chondrocranium of *Calotes versicolor* (Daud.) with a description of the osteocranium of a just-hatched young. *Quarter J Microscopical Sci.* 1946;s2-87(347):237-297.
46. Visser JGJ. Ontogeny of the chondrocranium of the chamaeleon, *Microsaura pumila pumila* (Daudin). *Annals of the University of Stellenbosch.* 1972;47A(2):1-68.
47. Brock GT. The skull of the chameleon, *Lophosaura ventralis* (gray); some developmental stages. *Proceedings of the Zoological Society of London.* 1940;B110(3-4):219-241. <https://doi.org/10.1111/j.1469-7998.1940.tb00037.x>.
48. Rieppel O. Über die Entwicklung des Basicranium bei *Chelydra serpentina* Linnaeus (Chelonia) und *Lacerta sicula* Rafinesque (Lacertilia). *Verhandlungen der Naturforschenden Gesellschaft in Basel.* 1977;86:153-170.
49. Rieppel O. Die orbitotemporale Region im Schädel von *Chelydra serpentina* Linnaeus (Chelonia) und *Lacerta sicula* Rafinesque (Lacertilia). *Acta Anat.* 1976;96(3):309-320. <https://doi.org/10.1159/000144683>.
50. El-Toubi MR, Kamal AM. The development of the skull of *Ptyodactylus hasselquistii*. I. The development of the chondrocranium. *J Morphol.* 1961;108(1):63-93. <https://doi.org/10.1002/jmor.1051080104>.
51. Kamal AM. The chondrocranium of *Hemidactylus turcica*. *Anat Anzeiger.* 1961;109:109-113.
52. Kamal AM. The chondrocranium of *Tropicolotes tripolitanus*. *Acta Zoologica.* 1960;41(3):297-312. <https://doi.org/10.1111/j.1463-6395.1960.tb00482.x>.
53. Hüppi E, Sánchez-Villagra MR, Tzika AC, Werneburg I. Ontogeny and phylogeny of the mammalian chondrocranium: the cupula nasi anterior and associated structures of the anterior head region. *Zool Lett.* 2018;4(29):29. <https://doi.org/10.1186/s40851-018-0112-0>.
54. Werneburg I, Yaryhin O. Character definition and tempus optimum in comparative chondrocranial research. *Acta Zool.* 2019; 100(4):376-388. <https://doi.org/10.1111/azo.12260>.
55. Kaucka M, Petersen J, Tesarova M, et al. Signals from the brain and olfactory epithelium control shaping of the mammalian nasal capsule cartilage. *eLife.* 2018;13:7. <https://doi.org/10.7554/eLife.34465>.
56. Bellairs AA. Observations on the cranial anatomy of *Anniella*, and a comparison with that of other burrowing lizards. *Proc Zool Soc London.* 1950;119(4):887-904. <https://doi.org/10.1111/j.1096-3642.1950.tb00915.x>.
57. Kuratani S, Ahlberg PE. Evolution of the vertebrate neurocranium: problems of the premandibular domain and the origin of the trabecula. *Zoological Lett.* 2018;4(1):1. <https://doi.org/10.1186/s40851-017-0083-6>.
58. Kuratani S. The neural crest and origin of the neurocranium in vertebrates. *Genesis.* 2018;56(6-7):e23213. <https://doi.org/10.1002/dvg.23213>.
59. Kovtun MF, Yarygin A. Formation of the orbito-temporal region of chondrocranium in embryogenesis of the sand lizard, *Lacerta agilis* (Reptilia, Squamata). *Vestnik Zool.* 2010;44:327-336.
60. Yarygin AN. Formation of parachordals, acrochordal cartilage and trabecula cranii in the skull of the sand lizard, *Lacerta agilis* (Reptilia, Squamata). *Vestnik Zool.* 2009;43(4):315-320.
61. Yarygin AN. Development of pterygoquadrate complex in the embryogenesis of sand lizard, *Lacerta agilis* (Reptilia, Squamata). *Vestnik Zool.* 2010;44(2):107-114. <https://doi.org/10.2478/v10058-010-0008-8>.
62. Yaryhin O, Klembara J. Different embryonic origin of the basiptyergoid process in two species of *Lacerta* (Squamata):

- Lacertidae). *Biologia*. 2015;70(4):530-534. <https://doi.org/10.1515/biolog-2015-0058>.
63. Hedges SB, Marin J, Suleski M, Paymer M, Kumar S. Tree of life reveals clock-like speciation and diversification. *Mol Biol Evol*. 2015;32(4):835-845. <https://doi.org/10.1093/molbev/msv037>.
  64. Crawford NG, Parham JF, Sellas AB, et al. A phylogenomic analysis of turtles. *Mol Phylogenet Evol*. 2015;83:250-257. <https://doi.org/10.1016/j.ympev.2014.10.021>.
  65. Müller F. Zur embryonalen Kopfentwicklung von *Crocodylus cataphractus* Cuv. *Rev Suisse Zool*. 1967;74:189-294. <https://doi.org/10.5962/bhl.part.75851>.
  66. Schauinsland HH. *Sphenodon, Callorhynchus, Chamaleo, Beiträge zur Entwicklungsgeschichte und Anatomie der Wirbeltiere*. Zoologica. Original Abhandlungen aus dem Gesamtgebiete der Zoologie.16 (Heft 39). Stuttgart: E. Nägeli; 1903:1-98. <https://www.biodiversitylibrary.org/bibliography/11952#/summary>.
  67. Sheil CA, Zaharewicz K. Anatomy of the fully formed chondrocranium of *Podocnemis unifilis* (Pleurodira: Podocnemididae). *Acta Zool*. 2014;95(3):358-366. <https://doi.org/10.1111/azo.12033>.
  68. Paluh DJ, Sheil CA. Anatomy of the fully formed chondrocranium of *Emydura subglobosa* (Chelidae): a pleurodiran turtle. *J Morphol*. 2013;274(1):1-10. <https://doi.org/10.1002/jmor.20070>.
  69. Kuratani S. Development of the chondrocranium of the loggerhead turtle, *Caretta caretta*. *Zool Sci*. 1999;16(5):803-818. <https://doi.org/10.2108/zsj.16.803>.
  70. Klembara J. Ontogeny of the partial secondary wall of the otoccipital region of the endocranium in prehatching *Alligator mississippiensis* (Archosauria, Crocodylia). *J Morphol*. 2005;266(3):319-330. <https://doi.org/10.1002/jmor.10380>.
  71. Brock GT. The skull of *Acontias meleagris*, with a study of the affinities between lizards and snakes. *J Linn Soc London, Zool*. 1941;41(277):71-88. <https://doi.org/10.1111/j.1096-3642.1941.tb02289.x>.
  72. Montero R, Gans C, Luisa LM. Embryonic development of the skeleton of *Amphisbaena darwini heterozonata* (Squamata: Amphisbaenidae). *J Morphol*. 1999;239(1):1-25. [https://doi.org/10.1002/\(SICI\)1097-4687\(199901\)239:1<1::AID-JMOR1>3.0.CO;2-A](https://doi.org/10.1002/(SICI)1097-4687(199901)239:1<1::AID-JMOR1>3.0.CO;2-A).
  73. Bellairs AD. Orbital cartilages in snakes. *Nature*. 1948;162(4133):106.
  74. Bellairs A'A, Gans C. A reinterpretation of the amphisbaenian orbitosphenoid. *Nature*. 1983;302(5905):243-244. <https://doi.org/10.1038/302243a0>.
  75. Lobo I. Pleiotropy: one gene can affect multiple traits. *Nature Education*. 2008;1:10.
  76. Wilkie AO. Why study human limb malformations? *J Anat*. 2003;202(1):27-35. <https://doi.org/10.1046/j.1469-7580.2003.00130.x>.
  77. Chokdeemboon C, Mahatumarat C, Rojvachiranonda N, Tongkobetch S, Suphapeetiporn K, Shotelersuk V. FGFR1 and FGFR2 mutations in Pfeiffer syndrome. *J Craniofac Surg*. 2013;24(1):150-152. <https://doi.org/10.1097/SCS.0b013e3182646454>.
  78. Cai J, Goodman BK, Patel AS, et al. Increased risk for developmental delay in Saethre-Chotzen syndrome is associated with TWIST deletions: an improved strategy for TWIST mutation screening. *Hum Genet*. 2003;114(1):68-76. <https://doi.org/10.1007/s00439-003-1012-7>.
  79. Cornejo-Roldan LR, Roessler E, Muenke M. Analysis of the mutational spectrum of the FGFR2 gene in Pfeiffer syndrome. *Hum Genet*. 1999;104(5):425-431. <https://doi.org/10.1007/s004390050979>.
  80. Alessandri JL, Dagonneau N, Laville JM, Baruteau J, Hebert JC, Cormier-Daire V. RAB23 mutation in a large family from Comoros Islands with carpenter syndrome. *Am J Med Genet A*. 2010;152A(4):982-986. <https://doi.org/10.1002/ajmg.a.33327>.
  81. Graf D, Malik Z, Hayano S, Mishina Y. Common mechanisms in development and disease: BMP signaling in craniofacial development. *Cytokine Growth Factor Rev*. 2016;27:129-139. <https://doi.org/10.1016/j.cytogfr.2015.11.004>.
  82. Pignatti E, Zeller R, Zuniga A. To BMP or not to BMP during vertebrate limb bud development. *Semin Cell Dev Biol*. 2014;32:119-127. <https://doi.org/10.1016/j.semcdb.2014.04.004>.
  83. Litingtung Y, Dahn RD, Li Y, Fallon JF, Chiang C. Shh and Gli3 are dispensable for limb skeleton formation but regulate digit number and identity. *Nature*. 2002;418(6901):979-983. <https://doi.org/10.1038/nature01033>.
  84. Hirasawa T, Kuratani S. Evolution of the vertebrate skeleton: morphology, embryology, and development. *Zoological Lett*. 2015;1(2):2. <https://doi.org/10.1186/s40851-014-0007-7>.
  85. Gans C, Northcutt RG. Neural crest and the origin of vertebrates: a new head. *Science*. 1983;220(4594):268-273. <https://doi.org/10.1126/science.220.4594.268>.
  86. Couly GF, Coltey PM, Le Douarin NM. The triple origin of skull in higher vertebrates: a study in quail-chick chimeras. *Development*. 1993;117(2):409-429.
  87. Olsson L, Ericsson R, Cerny R. Vertebrate head development: segmentation, novelties, and homology. *Theory Biosci*. 2005;124(2):145-163. <https://doi.org/10.1007/BF02814481>.
  88. Werneburg I, Maier W, Joyce WG. Embryonic remnants of intercentra and cervical ribs in turtles. *Biol Open*. 2013;2(11):1103-1107. <https://doi.org/10.1242/bio.20135439>.
  89. Hunt P, Gulisano M, Cook M, et al. A distinct Hox code for the branchial region of the vertebrate head. *Nature*. 1991;353(6347):861-864. <https://doi.org/10.1038/353861a0>.
  90. Bohmer C, Werneburg I. Deep time perspective on turtle neck evolution: chasing the Hox code by vertebral morphology. *Sci Rep*. 2017;7(1):8939. <https://doi.org/10.1038/s41598-017-09133-0>.
  91. Steedman HF. Alcian blue 8GS: a new stain for Mucin. *Quarter J Micros Sci Royal Micros Soc, Trans*. 1950;91(4):477-479.
  92. Oelrich TM. *The Anatomy of the Head of Ctenosaura pectinata (Iguanidae)*. Ann Arbor: University of Michigan Museum of Zoology; 1956:122.

## SUPPORTING INFORMATION

Additional supporting information may be found online in the Supporting Information section at the end of this article.

**How to cite this article:** Yaryhin O, Klembara J, Pichugin Y, Kaucka M, Werneburg I. Limb reduction in squamate reptiles correlates with the reduction of the chondrocranium: A case study on serpentiform anguils. *Developmental Dynamics*. 2021;250:1300-1317. <https://doi.org/10.1002/dvdy.307>